

Variability in the freshwater balance of northern Marguerite Bay, Antarctic Peninsula: results from $\delta^{18}\text{O}$

Michael P. Meredith^{1*}, Mark A. Brandon², Margaret I. Wallace¹, Andrew Clarke¹,
Melanie J. Leng³, Ian A. Renfrew⁴, Nicole P.M. van Lipzig⁵, John C. King¹

¹ British Antarctic Survey, High Cross, Madingley Road, Cambridge, U.K.

² Department of Earth Sciences, The Open University, Milton Keynes, U.K.

³ NERC Isotope Geosciences Laboratory, British Geological Survey, Nottingham, U.K. and
School of Geography, University of Nottingham, Nottingham, U.K.

⁴ School of Environmental Sciences, University of East Anglia, Norwich, U.K.

⁵ Physical and Regional Geography Research Group, Katholieke Universiteit Leuven, Belgium

* corresponding author. Tel: +44-1223-221586. Fax: +44-1223-221226. Email: mmm@bas.ac.uk

Abstract

We investigate the seasonal variability in freshwater inputs to the Marguerite Bay region (Western Antarctic Peninsula) using a time series of oxygen isotopes in seawater from samples collected in the upper mixed layer of the ocean during 2002 and 2003. We find that meteoric water, mostly in the form of glacial ice melt, is the dominant freshwater source, accounting for up to 5% of the near-surface ocean during the austral summer. Sea ice melt accounts for a much smaller percentage, even during the summer (maximum around 1%). The seasonality in meteoric water input to the ocean (around 2% of the near-surface ocean) is not dissimilar to that of sea ice melt (around 2% in 2002 and 1% in 2003), contradicting the assumption that sea ice processes dominate the seasonal evolution of the physical ocean environment close to the Antarctic continent. Three full-depth profiles of oxygen isotopes collected in successive Decembers (2001, 2002 and 2003) indicate that around 4 m of meteoric water is present in the water column at this time of year, and around 1 m of sea ice formed from this same water column. The predominance of glacial melt is significant, since it is known to be an important factor in the operation of the ecosystem, for example by providing a source of nutrients and modifying the physical environment to control the spatial extent and magnitude of phytoplankton blooms.

The Western Antarctic Peninsula is undergoing a very rapid change in climate, with increasing ocean and air temperatures, retreating glaciers and increases in precipitation associated with changes in atmospheric circulation. As climate change continues, we expect meteoric water inputs to the adjacent ocean to rise further. Sea ice in this sector of the Antarctic has shown a climatic decrease, thus we expect a reduction in oceanic sea ice melt fractions if this change continues. Continued monitoring of the oceanic freshwater budget at the western Peninsula is

needed to track these changes as they occur, and to better understand their ecological consequences.

Keywords: Antarctic Peninsula, Southern Ocean, Freshwater, Oxygen Isotopes, Sea Ice, Glacial Ice, Precipitation

1. Introduction

During the second half of the twentieth century, the Western Antarctic Peninsula (WAP; Figure 1) underwent the most dramatic warming of any region in the Southern Hemisphere (Vaughan *et al.*, 2003). Mean annual air temperatures here increased by nearly 3°C during this period, with the warming concentrated predominantly in the austral fall and winter (King and Harangozo, 1998; Turner *et al.*, 2005). Whilst some studies have linked a warming in this region to a change in the large-scale atmospheric circulation (in particular, a strengthening of the polar vortex, e.g. Thompson and Solomon (2002), an explanation for the full magnitude and seasonality of the observed warming remains elusive.

A paucity of reliable information on atmospheric circulation prior to the availability of satellite temperature sounder data in the late 1970s has hampered studies seeking to elucidate the causes and nature of the WAP warming. However, recent data have shown a strong correlation between atmospheric circulation in this region and WAP temperatures. Anomalously cyclonic conditions have been observed to be associated with warmer WAP winters as a result of increased warm air advection. Conversely, anomalously anticyclonic conditions have been observed to be associated with colder WAP winters caused by a decrease in warm air advection (Turner *et al.*, 1997). Accordingly, it seems likely that the trend toward higher WAP temperatures has been accompanied by a shift toward more cyclonic atmospheric circulation. The observed increase in precipitation at WAP stations during the period 1956-1992 is consistent with such a shift (Turner *et al.*, 1997).

The warming over the Antarctic Peninsula has had a profound influence on the ice sheet. A recent study showed that the majority of glaciers retreated during the past 50 years, and that average retreat rates are accelerating (Cook et al., 2005). It has also been shown that the annual duration of melting conditions has increased markedly on the Antarctic Peninsula (Vaughan, 2006). Whilst the majority of the increased meltwater will be refrozen within the ice sheet, there are indications that the increased runoff will make a significant contribution to global sea level rise (Vaughan, 2006).

Significant changes have also been observed in sea ice adjacent to the WAP. A long-term reduction in sea ice extent in the Bellingshausen Sea has been inferred, based on comparisons of modern data with earlier (sparse) data from ship observations during the middle of the twentieth century (King and Harangozo, 1998). The Bellingshausen Sea has also undergone a shortening of the sea ice season during the satellite era (Jacobs and Comiso, 1993; Parkinson, 2002).

Relatively little is known concerning the role of the ocean in this WAP climate change. There are indications of a large-scale warming of the deep waters of the Southern Ocean (Gille, 2002), some of which intrude onto the shelf in modified form, and studies have shown that melt rates of glaciers can depend strongly upon the temperature of marine waters impacting on them (Shepherd et al., 2004). However, the hypothesised link between changing ocean and glacial conditions is not yet proven. Observations of changing properties in the WAP and Bellingshausen Sea regions during the second half of the twentieth century have shown a profound warming of the summer ocean surface, of sufficient magnitude to have ecological consequences (Meredith

and King, 2005). There has also been a marked salinification of the summer ocean surface, caused by mixed layer processes driven by reduced sea ice formation (Meredith and King, 2005).

It is important to develop an understanding of the freshwater budget of the upper ocean adjacent to the WAP. At temperatures near the freezing point, seawater density depends almost entirely upon salinity. Accordingly, freshwater supplied to the ocean surface will act to strongly stabilise the water column, whilst sea ice formation (extraction of freshwater from the ocean surface) will destabilise the upper ocean and lead to deeper mixed layers (Meredith *et al.*, 2004; Smith and Klinck, 2002). Research in the WAP region has shown that water column stability and a shallow mixed layer are essential to phytoplankton bloom development (Mitchell and Holm-Hansen, 1991). Seasonal variability in the amount and spatial extent of glacial meltwater supplied to the ocean plays a critical role in oceanic ecosystem processes, and particularly primary production (Dierssen *et al.*, 2002). For example, adding a thin lens of freshwater to the ocean surface will greatly increase its stability, hence enabling phytoplankton to remain within a favourable light environment by preventing mixing to depths where light is a limiting factor. It should also be noted that glacial meltwater can be enriched in iron and other micronutrients, resulting from the glacial scouring of underlying rock surfaces and accumulation from atmospheric deposition (Dierssen *et al.*, 2002). It has been argued that increased runoff from melting glaciers as the Antarctic Peninsula continues to warm could lead to an increase in biomass in coastal waters, and a shift in phytoplankton assemblage composition (Dierssen *et al.*, 2002). It is known that in the WAP region, lower salinities are associated with a transition from a diatom-dominated system to one dominated by smaller cryptophytes, with potential consequences for the abundance of zooplankton populations (Moline *et al.*, 2000).

As well as being sensitive to climate variability itself, changes in the region west of the WAP can also drive variability in ocean properties at lower latitudes. Results from climate modelling studies have shown that the Bellingshausen Sea area, when “hosed” with additional freshwater inputs, can induce variability in ocean properties in the tropical Atlantic on decadal timescales, with oceanic advection being a key process (Hickey and Weaver, 2004).

Given the importance of freshwater to both physical and ecological dynamics west of the WAP and beyond, it is clearly desirable to maintain systematic monitoring capable of distinguishing the changing inputs to the ocean of freshwater from different sources, so that their effects (separately and combined) can be properly ascertained. In this paper, we present initial results from such a study, and comment on the implications of the observed levels and variability of the different freshwater inputs.

2. Background

2.1 Oceanographic context

The Southern Ocean Global Ocean Ecosystem Dynamics (SO GLOBEC) fieldwork area is centred on the central section of the WAP shelf, including Marguerite Bay (Figures 1, 2). Marguerite Bay is open to the west, bounded to the north and south by Adelaide Island and Alexander Island respectively, and closed to the east by the Antarctic Peninsula. The WAP shelf is typically around 450 m deep, with a deep trough, dubbed the Marguerite Trough, running into

Marguerite Bay from the shelf edge. Maximum depths of around 1600 m are found close to Alexander Island (Figure 2).

The water mass structure over the WAP continental shelf and in Marguerite Bay is relatively straightforward, and has been described in detail previously (Hofmann *et al.*, 1996; Klinck *et al.*, 2004; Meredith *et al.*, 2004; Smith *et al.*, 1999). The oceanic source for all other water masses found here is Circumpolar Deep Water (CDW). This is the voluminous, mid-depth water mass of the Antarctic Circumpolar Current (ACC), the southern boundary of which flows northeastward close to the WAP shelf slope. CDW can intrude onto the WAP shelf in certain locations, and it is believed that deep troughs that cross the shelf break (e.g. the Marguerite Trough) are important for this transfer. Unlike many other Antarctic shelf regions, there is no Antarctic Slope Front at the outer shelf break and slope (Jacobs, 1991; Whitworth *et al.*, 1998); consequently there is no dynamic barrier to the flow of CDW onto the shelf (Talbot, 1988). Momentum advection and curvature of the shelf break are important in driving CDW onto the shelf, following which the general shelf circulation can draw the CDW into the interior (Dinniman and Klinck, 2004). In a study of CDW intrusion onto the shelf along Marguerite Trough, it was deduced that the inflow is episodic, and that 4-6 events can occur in a year (Klinck *et al.*, 2004).

CDW typically has potential temperatures of 1.0-2.0°C and salinities of 34.60-34.74. It is usually considered as being comprised of two separate water masses, namely Upper CDW (UCDW), characterised by a relative maximum in potential temperature at a potential density of 27.72, and Lower CDW (LCDW), characterised by a relative maximum in salinity at a potential density of 27.80. UCDW is the form of CDW that dominates the deeper layers of the WAP shelf, though

LCDW has been observed in the deepest parts of some of the troughs (Klinck et al., 2004). The mechanisms by which LCDW intrudes onto the shelf are presently not well known.

A pycnocline separates the UCDW from the overlying Antarctic Surface Water (AASW). In winter, AASW is a relatively thick layer (typically 50-100 m) of cold water, with temperatures close to the freezing point and salinities around 33.5-34.0. During summer, ice melt freshens the very surface of this layer, which is also warmed by insolation. This warmer, fresher layer is undercut by the remnant of the deep winter mixed layer; this is termed Winter Water (WW) (Mosby, 1934; Toole, 1981), and is characterised by a minimum in potential temperature.

Modification of the shelf UCDW can be explained by a combination of across-shelf diffusion of heat and salt from offshore UCDW and vertical diffusion of heat and salt across the permanent pycnocline into the WW layer (Smith et al., 1999); this does not, however, preclude variability in the advective transfer of UCDW onto the shelf. Diffusive-convective instability is thought to be important for the upward heat flux across the pycnocline, and it is believed that the UCDW intrusions onto the shelf are important in both the heat and salt budgets of the area (Smith and Klinck, 2002). They are also likely to be ecologically important.

Circulation on the WAP shelf includes a coastal current that flows southwest along the west coast of Adelaide Island and into Marguerite Bay, then around the bay before exiting near Alexander Island (Beardsley *et al.*, 2004; Klinck *et al.*, 2004; Moffat *et al.*, 2007). Its pathway through Marguerite Bay is, however, difficult to trace (Moffat *et al.*, 2007). It is believed that this coastal

current may result from seasonal buoyancy forcing, primarily due to the input of coastal runoff at the western flank of the WAP (Moffat *et al.*, 2007).

There is marked interannual variability in water mass properties in the region. For example, it has been shown that ocean properties in northern Marguerite Bay show variability in response to atmospheric and cryospheric forcing associated with the El Niño / Southern Oscillation (ENSO) phenomenon (Meredith *et al.*, 2004). An especially deep winter mixed layer was observed in response to the strong 1997/98 El Niño event. This produced a deep (~150 m) and saline (~34.0) variety of WW that persisted into the following summer, with putative biogeochemical and ecological consequences (see Meredith *et al.* (2004) and Clarke *et al.* (2007) for discussion). Consideration of the forcings indicated that the scale of the ocean response to El Niño covered a broader spatial area than just the northern part of Marguerite Bay, though it was not possible to determine its full extent.

2.2 Sea ice characteristics

The northern part of Marguerite Bay is a seasonally ice covered region. Observations of ice cover available from passive microwave satellite sensors, such as the SSM/I, show Marguerite Bay typically ice-free (or with low concentrations) from December to March, although the start and end dates of the ice-free period can vary from November to January and March to May respectively. The presence of Rothera Research Station on Adelaide Island at the northern head of Marguerite Bay (Figures 1, 2) facilitates year-round *in situ* observations of sea ice concentration and type. Observations have been archived since 1997, and are summarised in

Figure 3. They are split into several subsidiary bays: Ryder Bay (where the oceanographic time series is taken) being the most comprehensively archived, although observations for Jenny Bay, South Cove and Hanger Cove are also available. Ryder Bay is typically largely covered in fast ice from June to September. There are typically periods of weeks where the fast ice cover is 10/10ths, interspersed with periods of a few days of lower concentration where there is clear water or brash ice. Ice free conditions and days with small concentrations of brash ice dominate the rest of the year; it is unusual for there to be multi-year ice.

There are sporadic measurements of ice thickness available for Ryder Bay, though by logistical necessity these are only made on “safe” areas of fast sea ice. Depths are typically 0.5 m during the late winter. In heavy ice years, such as 2002, the fast ice can last from May to November, whereas in light ice years, such as 1998, the periods of persistent fast ice can be as short as a few days. Meredith et al. (2004) show time series of monthly-mean sea ice fraction (independent of ice type) for 1998 to 2002 (their Figure 9). They also describe calculations of ice production, based on a simple 1-dimensional surface energy balance model, which uses primarily *in situ* meteorological and sea ice observations to calculate ice production amounts. Their Figures 12 and 17 illustrate that around 0.01 m of sea ice per day are produced during the freezing season; accumulating to (on average) 1.9 m per year.

2.3 Oxygen isotopes as oceanographic tracers

Whilst measurements of salinity are often sufficient to quantify total freshwater input to the ocean, they cannot elucidate the relative contributions from different freshwater sources: other

tracers are required for this. The ratio of oxygen isotopes in seawater (H_2^{18}O to H_2^{16}O) is especially useful in this context (Craig and Gordon, 1965). In general, $\delta^{18}\text{O}$ (the sample ratio of H_2^{18}O to H_2^{16}O referenced to the international standard, Vienna Standard Mean Ocean Water (VSMOW)) at the surface of the ocean is increased by evaporation and decreased by precipitation. Away from the surface, $\delta^{18}\text{O}$ is a conservative tracer. In these contexts, it is similar to salinity as an ocean tracer. Indeed, it is well known that the surface of much of the world ocean shows a quasi-linear relationship between salinity and $\delta^{18}\text{O}$, with the slope depending on the evaporation/precipitation characteristics of the regions under study.

Unlike salinity, however, $\delta^{18}\text{O}$ in precipitation decreases with increasing latitude due to its correlation with temperature. High-latitude precipitation is isotopically light (i.e. depleted in the heavier H_2^{18}O molecule), with $\delta^{18}\text{O}$ values as low as $-50\text{\textperthousand}$ reported (Weiss *et al.*, 1979). The isotopically light nature of glacial ice (which is formed from high-latitude precipitation) has proved valuable in tracing the input of glacial ice melt to the Antarctic Bottom Water that forms on the shelves of the continent (e.g. Schlosser *et al.*, 1990; Schlosser *et al.*, 1991; Weiss *et al.*, 1979; Weppernig *et al.*, 1996). A second important difference between salinity and $\delta^{18}\text{O}$ is their behaviours during sea ice formation and melting. Ocean salinity is strongly affected by these processes, as a result of brine rejection or freshwater addition. However, $\delta^{18}\text{O}$ is only very marginally affected by these processes, with the fractionation factor for ice in equilibrium with seawater being of order 1.0026 to 1.0035 (Lehmann and Siegenthaler, 1991; Macdonald *et al.*, 1995; Majoube, 1971). The small isotope difference between sea ice and the surface water from which it formed has been used in various studies to distinguish sea ice melt from meteoric freshwater input (i.e. from freshwater deriving from the atmosphere), which is isotopically much

lighter at high latitudes (e.g. Bauch *et al.*, 1995; Jacobs *et al.*, 1985; Meredith *et al.*, 1999; Meredith *et al.*, 2001; Schlosser *et al.*, 1994). We use $\delta^{18}\text{O}$ data here in this context.

3. Methods

Since late 1997, the British Antarctic Survey (BAS) has been conducting the Rothera Oceanographic and Biological Time Series (RaTS) project in Ryder Bay, close to the BAS Research Station at Rothera on Adelaide Island (Figure 2). As part of RaTS, a Chelsea Instruments Aquapack Conductivity-Temperature-Depth (CTD) instrument was used to profile the upper-ocean characteristics up to the end of 2002. The instrument package was lowered and raised using a hand-cranked winch, with casts limited to a maximum depth of 200 m by the pressure rating of the instrument (water depth at the sampling site is approximately 400 m). In early 2003, this instrument was replaced by a SeaBird SBE19, the higher pressure rating of which has enabled profiling that approaches the seabed. Both instruments were operated in self-recording mode, with data downloaded immediately after collection at Rothera. Casts were conducted from an inflatable boat during the ice-free months of the austral summer, and through a hole cut in the sea ice during the austral winter.

Precision of the CTD data was maintained by performing concurrent casts with SeaBird 911*plus* CTDs during the regular visits of *RRS James Clark Ross* and *ARSV Laurence M. Gould* to Rothera. The SeaBird salinity data were themselves calibrated using discrete samples measured on a Guildine Autosal 8400B salinometer, standardised with International Association for the

Physical Sciences of the Ocean (IAPSO) P-series standard seawater. Offsets to the Aquapack and SBE19 salinity data were applied to reconcile them with the calibrated SeaBird 911*plus* data.

In addition to the RaTS CTD casts, discrete water samples were taken from 15 m depth at the RaTS site using a Niskin bottle closed with a brass messenger. These samples have been used for a range of purposes, including measurements of size-fractionated chlorophyll and macronutrient concentrations. Since early 2002, samples from these Niskin bottles have also been drawn for oxygen isotope analysis; here we use data from the years 2002 and 2003. These samples were stored in 150 ml medical flat bottles with rubber inserts in the caps; these were sealed with Parafilm to prevent evaporation. Batches of oxygen isotope samples were transported annually (held at +4°C in the dark) to the Natural Environment Research Council Isotope Geosciences Laboratory (NIGL, Keyworth, U.K.). The waters were analysed for isotopes using the equilibration method for oxygen (Epstein and Mayeda, 1953) and a VG Isoprep 18 and Sira 10 mass spectrometer. During CTD casts performed from *RRS James Clark Ross*, the opportunity was taken to collect several samples from different depth levels, to better elucidate the vertical distribution of the different freshwater components; these vertical profiles of $\delta^{18}\text{O}$ were obtained in successive Decembers of 2001, 2002 and 2003. These samples were stored and transported in an identical fashion to the RaTS time series samples. All samples were analysed in triplicate to ensure data integrity; average precision of these samples is better than $\pm 0.02\text{\textperthousand}$. Data are available upon request by contacting the authors.

4. Results

4.1 Profiles and time series

Figure 4 shows the vertical profiles of salinity and $\delta^{18}\text{O}$ obtained during the Decembers of 2001, 2002 and 2003. The profiles show a broadly similar structure, with the deepest water present representing the upper layer of CDW. This is saline compared with the overlying waters (approximately 34.62), and relatively isotopically heavy (i.e. relatively enriched in the heavier H_2^{18}O molecule) with $\delta^{18}\text{O}$ values of approximately $-0.08\text{\textperthousand}$. Above this, the profiles become fresher and isotopically lighter toward the surface, where values are around 33.7 to 33.8 in salinity, and -0.55 to $-0.60\text{\textperthousand}$ in $\delta^{18}\text{O}$. That the surface waters are both fresh and isotopically light compared with CDW indicates that these waters contained significant meteoric water, not solely sea ice melt. The similarity of the profiles might be taken to suggest minimal interannual variability over this period; however, data with a higher frequency of sampling are needed to avoid aliasing problems.

The RaTS CTD time series of salinity, potential temperature and density for the upper 200 m of the water column are shown in Figure 5. For reference, the deeper CTD profiles with full-depth $\delta^{18}\text{O}$ data (conducted from *RRS James Clark Ross* and shown in Figure 4) were performed at the start, middle and end of the sequence shown in Figure 5. The data show seasonal progressions of properties that are relatively typical of this location (e.g. Meredith et al., 2004), with freshest surface water during January-March (around 32.0 to 33.0), and most saline surface water during the austral fall and winter (August-October, around 33.5 to 33.9). Potential temperature is highest during December-February (typically 1-3°C), reaching the surface freezing point by June and remaining there until October/November. Density strongly resembles salinity, as a consequence of the equation of state being dominated by salinity at low temperatures. There is some evidence

of difference between the two years, particularly in the depth of the winter mixed layer, which is considerably deeper in 2003 compared with 2002. We believe this is due to variability in the large-scale atmospheric forcing of the system, and will discuss this separately.

Time series of salinity and potential temperature from 15 m depth in the RaTS CTD data during 2003 and 2003 are shown in Figure 6 (upper and middle panel). The seasonality is again obvious, with freshest and warmest waters during the austral summer, and high salinities and freezing-point temperatures during the austral winter. Figure 6 (lower panel) shows the corresponding series of $\delta^{18}\text{O}$ from samples collected at 15 m depth. This also shows a marked seasonal signal, with isotopically lightest values (down to -0.8 to $-0.9\text{\textperthousand}$) during the austral summer, and isotopically heaviest values (up to around $-0.5\text{\textperthousand}$) during the austral winter. This seasonality in $\delta^{18}\text{O}$ is a strong indication of seasonality in the meteoric water input to northern Marguerite Bay, since sea ice processes alone would induce seasonality in salinity, but not significantly in $\delta^{18}\text{O}$. Note that, even during winter, the $\delta^{18}\text{O}$ value at 15 m is still much lower than that of the underlying CDW (Figure 4), indicating that significant meteoric water remains in the upper layers of Marguerite Bay throughout the year.

4.2 Seasonal freshwater loci

Freshwater loci (the evolution in time of the salinity/ $\delta^{18}\text{O}$ relationship) form a useful way of determining the dominant processes and the temporal variability of their influence. The locus for the 2002 data from the RaTS sampling site is shown in Figure 7. For this diagram, data points have been colour-coded and labelled according to the time of year. Extrapolations between the

endpoint of CDW and the meteoric water endmembers (precipitation and glacial meltwater) are marked (dashed lines), along with an approximate median line. (Section 4.3 details the isotope characteristics of these freshwater sources in more detail). In Figure 7, mixing of Marguerite Bay surface water with CDW would move the data points diagonally upward, along the line toward CDW. Conversely, mixing with meteoric water would move the points diagonally downward, along the line toward fresher, isotopically lighter waters. Sea ice processes would move the data points almost horizontally on this diagram.

The cluster of data points for January (yellow) have salinities of around 33.0-33.4, and $\delta^{18}\text{O}$ values mostly between -0.6 and -0.7‰. If we consider the November/December 2002 conditions (black data points) to be broadly indicative of the likely conditions in late 2001 (for which we have no $\delta^{18}\text{O}$ data), the shift in the salinity- $\delta^{18}\text{O}$ characteristics from November/December to January would be partly horizontal (to the left) and partly diagonal (toward isotopically light freshwater), and thus a combination of addition of sea ice melt and an addition of meteoric water. The next cluster of points on the locus (February-May; green) represents the freshest and isotopically lightest data in the sequence, with salinities as low as 32.9 and $\delta^{18}\text{O}$ less than -0.85‰. The shift to this cluster is indicative of the addition of substantial quantities of meteoric water, but significantly no sea ice melt is involved (there is no extra horizontal shift relative to the meteoric water envelope lines). The transition to the next cluster (June/July; red) sees data points moving toward higher salinities and higher $\delta^{18}\text{O}$ values. The cluster moves horizontally out of the meteoric water envelope, thus we infer both that both freezing and mixing with CDW (as the mixed layer deepens) are important for this transition. The following transition to August-October (blue points) sees generally higher salinities (around 33.75) with little change in $\delta^{18}\text{O}$:

this mainly horizontal shift is indicative of the effect of sea ice formation. During November/December (black points), salinities and $\delta^{18}\text{O}$ values are concurrently at their highest (approximately 33.8 and $-0.5\text{\textperthousand}$ respectively).

The corresponding locus for 2003 is shown in Figure 8. Whilst there are strong similarities with that of 2002 (Figure 7), there are also clear differences. The locus is clustered much more tightly to the meteoric water envelope (dashed lines), indicating less variability in the prevalence of sea ice melt at 15 m throughout the year. Indeed, only parts of the August-October and November/December clusters lie outside the envelope. From November/December 2002 (Figure 7) there is a small, predominantly horizontal shift toward January 2003 (yellow cluster, Figure 8), indicative of small quantities of sea ice melt. Conversely, during the transition to February-May, the cluster of points remains close to the middle of the meteoric water envelope. This indicates addition of meteoric water, and minimal influence of sea ice processes. The locus between June/July and August-October 2003 (red and blue, Figure 8) lies predominantly (but not exclusively) within the meteoric water envelope, indicating mixing with CDW to be dominant process, but with some sea ice formation occurring also. More mixing with the underlying CDW in 2003 compared with 2002 is not unexpected, given the deeper winter mixed layer in 2003.

It is important to note that the tighter clustering of the data points to the meteoric water envelope in 2003, compared with 2002, indicates only that the sea ice prevalence was less variable at 15m depth during this year, it does not indicate that it was less significant in the water column as a whole. Given the deeper mixed layer in winter 2003, sea ice melt integrated over the mixed layer

could well be more significant in 2003. To fully address this, it is useful to first quantify the relative contributions from the freshwater sources.

4.3 Quantification of freshwater components

To quantify the relative prevalence of the respective freshwater contributors, we solved the three-component mass balance for each isotope sample collected:

$$f_{\text{cdw}} + f_{\text{sim}} + f_{\text{met}} = 1 \quad (1)$$

$$S_{\text{cdw}}, f_{\text{cdw}} + S_{\text{sim}}, f_{\text{sim}} + S_{\text{met}}, f_{\text{met}} = S \quad (2)$$

$$\delta_{\text{cdw}}, f_{\text{cdw}} + \delta_{\text{sim}}, f_{\text{sim}} + \delta_{\text{met}}, f_{\text{met}} = \delta \quad (3)$$

where:

$f_{\text{cdw}, (\text{sim}), [\text{met}]}$ is the derived fraction of UCDW, (sea ice melt), [meteoric water],

$S_{\text{cdw}, (\text{sim}), [\text{met}]}$ is the salinity of the UCDW, (sea ice melt), [meteoric water] endmember,

$\delta_{\text{cdw}, (\text{sim}), [\text{met}]}$ is the $\delta^{18}\text{O}$ of the UCDW, (sea ice melt), [meteoric water] endmember,

S is the measured salinity,

δ is the measured $\delta^{18}\text{O}$ value.

The choice of values for characteristics of the endmembers (i.e. the undiluted sources prior to their being mixed to form the waters that were sampled) is important in determining realistic fractions for the freshwater contributors. Most of these are already clearly established, but others (such as the average $\delta^{18}\text{O}$ of meteoric water) are less well known. We have instigated a program

of measuring these endmembers more thoroughly, but for the purposes of the present paper we have adopted the following values (summarized in Table 1). The meteoric water endmember salinity is set to 0. The CDW endmember salinity is set to 34.62; this is the deepest value obtained during the vertical profiling at the RaTS site. Note that this value does not represent “pure” CDW in the ACC, but rather best depicts the local variety to which freshwater is added. The CDW $\delta^{18}\text{O}$ is set to $-0.08\text{\textperthousand}$; again, this is the deepest value obtained during the vertical profiling at the RaTS site, and is used for the same reasons given above. The sea ice melt salinity endmember is set to 7, which is a representative value for the region under study. The $\delta^{18}\text{O}$ endmember value for sea ice is set to $+2.1\text{\textperthousand}$, derived as a realistic $\delta^{18}\text{O}$ value of the surface water for this area plus an offset to account for fractionation upon freezing.

The largest uncertainties are associated with the choice of $\delta^{18}\text{O}$ value for the meteoric water endmember. This is because it is a combination of local precipitation (which can have a large degree of variability if measured directly), and glacial ice melt. Glacial ice melt itself can be in the form of surface runoff, or melt from a glacier or ice shelf in direct contact with the ocean. Precipitation and glacial ice melt can have different $\delta^{18}\text{O}$ values, since precipitation that is incorporated into glaciers may have accumulated at different surface elevations and/or can have fallen during a time of different climatic conditions. The isotope values of the different terms in the mass balance of the northern end of George VI ice shelf (which calves into Marguerite Bay) were discussed previously by (Potter and Paren, 1985). They observed that the ice flux into the shelf had a $\delta^{18}\text{O}$ value of around $-20\text{\textperthousand}$, whereas direct accumulation onto the northern part of the ice shelf in the form of precipitation had a much higher $\delta^{18}\text{O}$ value, around $-13\text{\textperthousand}$. Accordingly, we have adopted a value of $-17\text{\textperthousand}$ as a reasonable mean $\delta^{18}\text{O}$ value of the meteoric endmember

in our freshwater balance, though with large associated uncertainty. Errors in the derived freshwater percentages resulting from uncertainty in choice of endmember (determined through sensitivity studies) and measurement error are typically around $\pm 1\%$.

The results of these calculations are shown in Figure 9, the upper curve of which shows the temporal evolution of the meteoric water percentage at 15 m depth, and the lower curve of which shows the corresponding sea ice melt percentages. Note that the sea ice melt percentages are frequently negative; this indicates that at the time of sampling, there had been a net sea ice formation from these waters. Meteoric water percentages vary between nearly 5% during the late austral summer and fall to less than 3% during the austral winter. Sea ice melt percentages vary between 0-1% during the austral summer, to -1 to -2% during the austral winter.

It should be noted that the meteoric water prevalence is always higher than the sea ice prevalence, demonstrating clearly the importance of meteoric water inputs at this location. The seasonality in the meteoric water is comparable to that in the sea ice melt (around 2% range in both years, compared with ~2% and 1% for sea ice melt in 2002 and 2003 respectively). This indicates that assumptions of freshwater seasonality being controlled predominantly by sea ice formation and melting in Antarctic coastal waters are not necessarily valid. We note that Ryder Bay, although being fairly open, is surrounded by glaciers which may have increased the glacial meltwater input at the RaTS site above that typical for the WAP shelf as a whole.

As observed above, the sea ice melt at 15 m is much less variable in 2003 compared with 2002. In particular, during the months July through October, the values for sea ice melt are around -0.5

to -1.0% in 2003, compared with around -1.5% in 2002. However, the mixed layer was much deeper in 2003, down to around 180 m in August and averaging around 120 m for July to October (Figure 5). During 2002, the mixed layer for the same period was approximately one third as deep, around 40 m. If we assume momentarily that the freshwater fractions derived for 15 m depth are spread equally over the full depth of the mixed layer, then the integrated sea ice melt percentages in 2003 become comparable to those in 2002, and very possibly larger.

We should note that the above calculation makes a number of assumptions, for example it ignores the possibility of changes in freshwater content beneath the mixed layer in the underlying pycnocline. With data from just one level (15 m), we cannot fully quantify the separate integrated freshwater components in the upper ocean as a function of time. However, using the full-depth profiles of $\delta^{18}\text{O}$ obtained from *RRS James Clark Ross* during the Decembers of 2001, 2002 and 2003, we can at least calculate the freshwater inventories at these times. To do this, we first calculated the relative freshwater percentages for these profiles using Equations 1-3 above. The results of this are shown in Figure 10, from which it can be seen that the meteoric water content greatly exceeds the sea ice melt content. Meteoric water content reaches 3% at the surface, whilst sea ice melt content at the surface is between -0.5 and -1.0% . To quantify the total freshwater components present in the water column at the time of sampling, we integrated the derived fractions with depth:

$$H_{\text{met}} = \int_{z_{\text{max}}}^0 f_{\text{met}} dz \quad (4)$$

$$H_{\text{sim}} = \int_{Z_{\text{max}}}^0 f_{\text{sim}} \, dz \quad (5)$$

where H_{met} is the column inventory of meteoric water,

H_{sim} is the column inventory of sea ice melt,

Z_{max} is the deepest level over which the profile is integrated.

The results of these calculations are shown in Figure 10. Meteoric water inventories were between around 4.0 and 4.5 m, with uncertainty of around 1 m. Sea ice melt inventories were around -1 m, with similar uncertainty. Accounting for the difference in density between water and ice (ratio of around 0.9), this would indicate that a net amount of around 1.1 m of sea ice had been formed from the water column at the time of sampling, although the uncertainty in this estimate is large. Note that this does not imply that sea ice of this thickness existed in Marguerite Bay at the time; rather it is indicative of the net thickness of sea ice that had formed from the water column up to the time it was sampled.

It is also important to note that the quantified prevalences of sea ice melt and meteoric water are from just one location, and previous observations (Meredith et al., 2004) indicate that oceanic advection is important in controlling the temporally-evolving properties in northern Marguerite Bay. The importance of advection to the freshwater budget of this area is seen further from calculations of local ice production per unit area, made with a one-dimensional model and using forcings derived from meteorological and sea-ice observations collected at the nearby Rothera Research Station. Details of the ice production model and its application to the Marguerite Bay region have been described previously (Meredith et al., 2004; Renfrew et al., 2002).

Annual ice production derived using this model was 2.97m in 2001, 0.98m in 2002, and 2.80m in 2003. The lower ice production in 2002 was primarily due to a generally high sea ice fraction during the winter months, which cut off further sea ice production, and also contributed to the relatively shallow mixed-layer (Figure 5) by limiting wind-induced oceanic mixing. Whilst the 2002 value agrees well with the isotope-derived value for ice formation of 1m, especially given the significant uncertainty in this value, the 2001 and 2003 values do not. The discrepancy arises because the model quantifies ice production at a single location, whereas the isotope-derived value inherently includes waters that are advected through the sampling area, and which may have received freshwater inputs at significant distances from the RaTS site. It has been demonstrated already that the RaTS hydrographic data show variability in response to changes in large-scale forcing and climate variability (Meredith et al., 2004), rather than changes in purely local conditions, and clearly this is equally significant for more exotic tracers such as oxygen isotopes. It is important to bear this in mind when interpreting the results presented here.

6. Discussion and Conclusions

Whilst the tracers we have used (salinity, $\delta^{18}\text{O}$) are not capable of distinguishing glacial ice melt separately from direct precipitation into the ocean, there are good reasons to suspect that the glacial ice melt component is the largest contributor to the meteoric water. For example, during 2002, there is a phase difference between the peak freshwater prevalences (Figure 9). The sea ice melt percentage peaked in late January, whereas the meteoric water did not peak until March. This indicates that the meteoric water was not dominated by snow that had accumulated on top of

the sea ice during winter, else they would have peaked at the same time. The difference in the times of peaking therefore reflects the time for maximum glacial runoff to reach the RaTS sampling site.

A further indication of the relative importances of glacial ice melt and precipitation in the meteoric water input to the ocean is provided from meteorological analyses. Note that measurements of precipitation in this region are sparse, and it is difficult to distinguish incident precipitation from blowing snow. Therefore, we instead examined the output of a regional atmospheric model, integrated for 7 years with a horizontal grid spacing of 14 km and realistically forced at the boundaries (Van Lipzig *et al.*, 2004). Figure 11 shows the precipitation averaged over Marguerite Bay; it can be seen that average precipitation into Marguerite Bay is of order 0.1 m per month (around 1.2 m annual average), with a significant semiannual term superposed. Whilst there is uncertainty concerning the rate at which this precipitation is mixed to deeper layers in the ocean or advected away from the region of input, this is significantly less than the column inventory of meteoric water measured at the RaTS site in December (around 4 m). This again suggests glacial ice melt to be the dominant source of meteoric water input.

The significant amounts of glacial ice melt input to the ocean has important consequences for both the physical and biological systems. The freezing point of water is a function of salinity, thus the input of glacial ice melt will act to influence further sea ice production. This will subsequently impact on local processes such as air-sea fluxes of heat, momentum, and so on. There are large-scale consequences also; for example, studies with coupled climate models have indicated that enhanced freshwater inputs to the region west of the Antarctic Peninsula can, over

long periods, induce changes in ocean temperature, salinity and isopycnal depth in the tropical Atlantic (Hickey and Weaver, 2004). Indeed, this mechanism was put forward as a possible explanation for an observed decadal mode of tropical Atlantic variability.

Glacial ice inputs are known to be important for ecosystem dynamics in Antarctic waters. Glacial meltwater can be enriched in iron and other micronutrients, and thereby constitute a source of essential trace micronutrients for offshore waters, with consequences for primary production there (Dierssen et al., 2002). Release of glacial meltwater will also act to stabilise the water column. This will have the action of retaining phytoplankton within a favourable light environment by reducing the depth of mixing, and it is known that water column stability and a shallow mixed layer are critical for phytoplankton bloom development in this region (Mitchell and Holm-Hansen, 1991). There will also be secondary consequences of a shallower mixed layer and larger concentrations of phytoplankton. For example, these factors will tend to restrict heat input from the atmosphere to shallower depths, by blocking the downward penetration of radiation and restricting the depth of mixing of warmed surface waters. This will tend to produce warmer surface waters, again with impacts on sea ice production and associated biogeochemical and ecological functions.

The seasonal cycles of meteoric water and sea ice melt fractions that we have derived represent the present-day situation at the western Peninsula, following at least 50 years of rapid regional climate change. As this change continues, the mean prevalence and seasonality in the freshwater fractions will undoubtedly change also. For example, the majority of glaciers on the Peninsula are retreating, and this retreat is accelerating (Cook et al., 2005). It is also known that the annual

melting period has been increasing at the Peninsula, at a rate of around half a day per year (Torinesi et al., 2003). These changes will act to increase the prevalence of meteoric water, and are also likely to increase the magnitude of its seasonality (c.f. Figure 9).

Although data from the pre-satellite era are sparse, indications are that the sea ice extent in the Bellingshausen Sea has decreased significantly since the 1950s (King and Harangozo, 1998). For the satellite era, various studies have shown geographically-significant patterns of sea ice changes. It has been shown that sea ice duration in the region west of the Peninsula has decreased in duration by around 1-2 days per year (Parkinson, 2002; Vaughan et al., 2003). It is worth noting that the atmospheric warming trend at the Peninsula is strongest during April-September, coinciding with the time of strongest sea ice formation. Overall, these changes (if continued) are likely to be represented as a “flattening” of the seasonal sea ice melt curve (c.f. Figure 9), with less positive sea ice melt during summer and less negative sea ice melt during winter. This accords well with observations of previous changes in surface ocean salinity in the Bellingshausen Sea during the second half of the last century (Meredith and King, 2005), where a strong summer salinification was observed, driven by mixed layer processes associated with reduced sea ice production. This summer salinification is equivalent to a long-term reduction in the summer prevalence of sea ice melt, and would be seen as a reduction in the seasonality of the sea ice melt curve (Figure 9).

It has been shown previously that winter mixed layer depths in the region of Marguerite Bay and the WAP depend critically on the rate of sea ice production (Meredith *et al.*, 2004; Smith and Klinck, 2002). The changes that have been observed at the WAP include a reduction in sea ice

formation; this will act to reduce the mixed layer depths, with likely impacts on biogeochemical processes and primary production.

Unlike many regions around Antarctica, the region west of the Antarctic Peninsula is not one where appreciable quantities of dense water are formed on the shelf. Consequently, for example, there are no major sources of Antarctic Bottom Water (AABW) in this sector of the Southern Ocean. However, downslope convection of dense water from the shelf has been observed occurring in front of Elephant Island, at the very tip of the Peninsula (Meredith et al., 2003), with subsequent ventilation of the deep CDW and AABW layers. Sea ice production is believed to be important to the production of this dense water, by adding salt to the shelf waters during winter. If the climate change continues in this region, extending to the tip of the Antarctic Peninsula, this mode of ventilating the deep Southern Ocean may be shut off.

We note that our time series reflects the temporal evolution of freshwater characteristics at just one location. However, it has been seen previously (and is reiterated here) that this location is sensitive to large-scale climate change and variability (Meredith et al., 2004), and we believe it is likely to give indications of conditions and processes at broader scales than purely local. The wintertime data we are able to acquire from this location makes the series especially valuable in monitoring the evolving physical and ecological systems, since this is when some of the key processes occur (sea ice production, mixed layer deepening, mixing with CDW etc.). As climate change continues at the WAP, monitoring programs such as RaTS will continue to track the ecosystem's response. Continued time series measurements of oxygen isotopes, using the

measurements presented here as a baseline, will enable determination of the changes in freshwater forcings, and the ecosystem changes that are induced in response.

Acknowledgements

We thank Rayner Piper, Andrew Miller and the Boating Officers at Rothera for undertaking the collection of data and samples used in this paper. Carol Arrowsmith undertook the isotope analysis. We thank Eileen Hofmann, Ian Allison and an anonymous reviewer for their useful input. This work was funded by the U.K. Natural Environment Research Council (NERC), and is U.S. GLOBEC contribution number 507.

References

Bauch, D., Schlosser, P., Fairbanks, R.G., 1995. Freshwater balance and the sources of deep and bottom waters in the Arctic Ocean inferred from the distribution of H₂¹⁸O. *Progress in Oceanography* 35, 53-80.

Beardsley, R.C., Limeburner, R., Owens, W.B., 2004. Drifter measurements of surface currents near Marguerite Bay on the western Antarctic Peninsula shelf during austral summer and fall, 2001 and 2002. *Deep-Sea Research II* 51, 1947-1964.

Clarke, A., Meredith, M.P., Wallace, M.I., Brandon, M.A., Thomas, D.N., 2007. Seasonal and interannual variability in temperature, chlorophyll and macronutrients in Ryder Bay, northern Marguerite Bay, Antarctica. *Deep-Sea Research II*, in press.

Cook, A.J., Fox, A.J., Vaughan, D.G., Ferrigno, J.G., 2005. Retreating Glacier Fronts on the Antarctic Peninsula over the Past Half-Century. *Science* 308 (5721), 541-544.

Craig, H., Gordon, L., 1965. Deuterium and oxygen-18 variations in the ocean and the marine atmosphere. In: Tongiorgio, E. (Ed.), *Stable isotopes in Oceanographic Studies and Paleotemperatures*, Spoleto, pp. 9-130.

Dierssen, H.M., Smith, R.C., Vernet, M., 2002. Glacial meltwater dynamics in coastal waters west of the Antarctic Peninsula. *Proceedings of the National Academy of Sciences* 99 (4), 1790-1795.

Dinniman, M.S., Klinck, J.M., 2004. A model study of circulation and cross-shelf exchange on the west Antarctic Peninsula continental shelf. Deep-Sea Research II 51, 2003-2022.

Epstein, S., Mayeda, T.K., 1953. Variation of ^{18}O content of waters from natural sources. Geochimica et Cosmochimica Acta 4, 213-224.

Gille, S.T., 2002. Warming of the Southern Ocean Since the 1950s. Science 295, 1275-1277.

Hickey, H., Weaver, A.J., 2004. The Southern Ocean as a source region for tropical Atlantic variability. Journal of Climate 20, 3960-3972.

Hofmann, E.E., Klinck, J.M., Lascara, C.M., Smith, D.A., 1996. Water mass distribution and circulation west of the Antarctic Peninsula and including Bransfield Strait. In: Ross, R.M. (Ed.), Foundations for Ecological Research West of the Antarctic Peninsula. American Geophysical Union, Washington D.C., pp. 61-80.

Jacobs, S.S., 1991. On the Nature and Significance of the Antarctic Slope Front. Marine Chemistry 35 (1-4), 9-24.

Jacobs, S.S., Comiso, J.C., 1993. A Recent Sea-Ice Retreat West of the Antarctic Peninsula. Geophysical Research Letters 20 (12), 1171-1174.

Jacobs, S.S., Fairbanks, R.G., Horibe, Y., 1985. Origin and evolution of water masses near the Antarctic continental margin: Evidence from $H_2^{18}O/H_2^{16}O$ ratios in sea water. In: Jacobs, S.S. (Ed.), Oceanology of the Antarctic Continental Shelf. American Geophysical Union, Washington D.C.

King, J.C., Harangozo, S.A., 1998. Climate change in the western Antarctic Peninsula since 1945: observations and possible causes. *Annals of Glaciology* 27, 571-575.

Klinck, J.M., Hofmann, E.E., Beardsley, R.C., Salighoglu, B., Howard, S., 2004. Water mass properties and circulation on the West Antarctic Peninsula continental shelf in austral fall and winter 2001. *Deep-Sea Research II* 51, 1925-1946.

Lehmann, M., Siegenthaler, U., 1991. Equilibrium oxygen- and hydrogen-isotope fractionation between ice and water. *Journal of Glaciology* 57, 23-26.

Macdonald, R.W., Paton, D.W., Carmack, E.C., Omstedt, A., 1995. The freshwater budget and under-ice spreading of Mackenzie River water in the Canadian Beaufort Sea based on salinity and $^{18}O/^{16}O$ measurements in water and ice. *Journal of Geophysical Research* 100 (C1), 895-919.

Majoube, M., 1971. Fractionnement en oxygène et en deutérium entre l'eau et sa vapeur. *Journal de Chimie et de Physique* 68, 1423.

Meredith, M.P., C.W. Hughes, Foden, P.R., 2003. Downslope convection north of Elephant Island, Antarctic Peninsula: Influence on deep waters and dependence on ENSO. *Geophysical Research Letters* 30 (9), 10.1029/2003GL017074.

Meredith, M.P., K.E. Grose, E.L. McDonagh, K.J. Heywood, R.D. Frew, Dennis, P.F., 1999. Distribution of oxygen isotopes in the water masses of Drake Passage and the South Atlantic. *Journal of Geophysical Research* 104 (C9), 20,949-920,962.

Meredith, M.P., K.J. Heywood, P.F. Dennis, L.E. Goldson, R.M.P. White, E. Fahrbach, U. Schauer, Østerhus, S., 2001. Freshwater fluxes through the western Fram Strait. *Geophysical Research Letters* 28 (8), 1615-1618.

Meredith, M.P., King, J.C., 2005. Rapid climate change in the ocean to the west of the Antarctic Peninsula during the second half of the twentieth century. *Geophysical Research Letters* 32 (L19604), 10.1029/2005GL024042.

Meredith, M.P., Renfrew, I.A., Clarke, A., King, J.C., Brandon, M.A., 2004. Impact of the 1997/98 ENSO on the upper waters of Marguerite Bay, western Antarctic Peninsula. *Journal of Geophysical Research* 109 (C9), 10.1029/2003JC001784.

Mitchell, B.G., Holm-Hansen, O., 1991. Observations and modeling of the Antarctic phytoplankton crop in relation to mixing depth. *Deep-Sea Research* 38, 981-1007.

Moffat, C., Beardsley, R., Owens, W.B., Van Lipzig, N., 2007. A first description of the Antarctic Peninsula Coastal Current. Deep-Sea Research II, in press.

Moline, M.A., Claustre, H., Frazer, T.K., Grzynski, J., Schofield, O., Vernet, M., 2000. Changes in phytoplankton assemblages along the Antarctic Peninsula and potential implications for the Antarctic food web. In: Davidson, E., Howard-Williams, C., Broady, P. (Eds.), Antarctic Ecosystems: Models for Wider Ecological Understanding. Cambridge University Press, pp. 263-271.

Mosby, H., 1934. The waters of the Atlantic Antarctic Ocean. Scientific Results of the Norwegian Antarctic Expedition, 1927-1928 11, 1-131.

Orsi, A.H., Smethie, W.M., Bullister, J.L., 2002. On the total input of Antarctic waters to the deep ocean: A preliminary estimate from chlorofluorocarbon measurements. Journal of Geophysical Research 107 (C8), 10.1029/2001JC000976.

Parkinson, C., 2002. Trends in the length of the Southern Ocean sea ice season, 1979-1999. Annals of Glaciology 34 (1), 435-440.

Potter, J.R., Paren, J.G., 1985. Interaction between ice shelf and ocean in George VI Sound, Antarctica. Oceanology of the Antarctic Continental Shelf. American Geophysical Union, pp. 35-58.

Renfrew, I.A., King, J.C., Markus, T., 2002. Coastal polynyas in the southern Weddell Sea: variability of the surface energy budget. *Journal of Geophysical Research* 107 (C6), 10.10129/12000JC000720.

Schlosser, P., Bayer, R., Foldvik, A., Gammelsrod, T., Rohardt, G., Munnich, K.O., 1990. Oxygen 18 and helium as tracers of Ice Shelf Water and water/ice interaction in the Weddell Sea. *Journal of Geophysical Research* 95, 3253-3263.

Schlosser, P., Bullister, J.L., Bayer, R., 1991. Studies of deep water formation and circulation in the Weddell Sea using natural and anthropogenic tracers. *Marine Chemistry* 35, 97-122.

Schlosser, P., D. Bauch, R. Fairbanks, Bonisch, G., 1994. Arctic river runoff: Mean residence time on the shelves and in the halocline. *Deep-Sea Research I* 41, 1053-1068.

Shepherd, A., Wingham, D., Rignot, E., 2004. Warm ocean is eroding West Antarctic Ice Sheet. *Geophysical Research Letters* 31 (L23402), 10.1029/2004GL021106.

Smith, D.A., Hofmann, E.E., Klinck, J.M., Lascara, C.M., 1999. Hydrography and circulation of the West Antarctic Peninsula Continental Shelf. *Deep-Sea Research I* 46, 925-949.

Smith, D.A., Klinck, J.M., 2002. Water properties on the west Antarctic Peninsula continental shelf: a model study of effects of surface fluxes and sea ice. *Deep-Sea Research II* 49, 4863-4886.

Talbot, M.H., 1988. Oceanographic environment of George VI Ice Shelf. *Annals of Glaciology* 11, 161-164.

Thompson, D.W.J., Solomon, S., 2002. Interpretation of recent Southern Hemisphere climate change. *Science* 296, 895-899.

Toole, J.M., 1981. Sea ice, winter convection and the temperature minimum layer in the Southern Ocean. *Journal of Geophysical Research* 86, 8037-8047.

Torinesi, O., Fily, M., Genthon, C., 2003. Interannual Variability and Trend of the Antarctic Ice Sheet Summer Melting Period from 20 Years of Spaceborne Microwave Data. *Journal of Climate* 16, 1047-1060.

Turner, J., Colwell, S.R., Harangozo, S., 1997. Variability of precipitation over the coastal western Antarctic Peninsula from synoptic observations. *Journal of Geophysical Research* 102, 13999-14007.

Turner, J., Colwell, S.R., Marshall, G.J., Lachlan-Cope, T.A., Carleton, A.M., Jones, P.D., Lagun, V., Reid, P.A., Iagovinka, S., 2005. Antarctic climate change during the last 50 years. *International Journal of Climatology* 25, 279-294.

Van Lipzig, N.P.M., King, J.C., Lachlan-Cope, T.A., van den Broeke, M.R., 2004. Precipitation, sublimation and snowdrift in the Antarctic Peninsula region from a regional atmospheric model. Journal of Geophysical Research 109 (D24106), 10.1029/2004JD004701.

Vaughan, D.G., 2006. Recent trends in melting conditions on the Antarctic Peninsula and their implications for ice-sheet mass balance and sea level. Arctic, Antarctic and Alpine Research 38 (1), 147-152.

Vaughan, D.G., Marshall, G.J., Connolley, W.M., Parkinson, C., Mulvaney, R., Hodgson, D.A., King, J.C., Pudsey, C.J., Turner, J., 2003. Recent rapid regional climate warming on the Antarctic Peninsula. Climatic Change 60 (3), 243-274.

Weiss, R.F., Ostlund, H.G., Craig, H., 1979. Geochemical studies of the Weddell Sea. Deep-Sea Research 26A, 1093-1120.

Weppernig, R., Schlosser, P., Khatiwala, S., Fairbanks, R.G., 1996. Isotope data from Ice Station Weddell: Implications for deep water formation in the Weddell Sea. Journal of Geophysical Research 101, 25,723-725,739.

Whitworth, T., Orsi, A.H., Kim, S.J., Nowlin, W.D., Locarnini, R.A., 1998. Water masses and mixing near the Antarctic Slope Front. In: Weiss, S.S.J.a.R.F. (Ed.), Ocean, Ice and Atmosphere: Interactions at the Antarctic Continental Margin. American Geophysical Union, Washington D.C., pp. 1-27.

Figure legends

Figure 1. Location of Marguerite Bay on the Western Antarctic Peninsula. The 1000, 2000 and 3000 m isobaths are marked.

Figure 2. Bathymetry of Marguerite Bay, from the recently compiled SO GLOBEC bathymetric dataset. Shading denotes depths deeper than 1500 m (darkest), 1500-500 m, 500-250 m and shallower than 250 m (lightest). Marked are the British Antarctic Survey research station at Rothera on Adelaide Island, and the location of the Rothera Time Series (RaTS) sampling site in Ryder Bay.

Figure 3. Winter fast-ice in Ryder Bay, northern Marguerite Bay, 1997-2006. Ice score ranges from 0 (open water) to 10 (complete fast ice cover). Data are plotted for the calendar year, so that winter lies in the centre of the plot. Figure reproduced from Clarke *et al.* (2007).

Figure 4: Vertical profiles of $\delta^{18}\text{O}$ and salinity obtained by CTD casts at the RaTS site conducted from *RRS James Clark Ross* during December 2001 (red), December 2002 (black) and December 2003 (blue).

Figure 5: Time series of salinity, potential temperature ($^{\circ}\text{C}$) and density (σ_0 ; kg/m^3) for the upper 200 m of the water column during 2002 and 2003, from CTD casts conducted at the RaTS site.

Figure 6: Time series of salinity, potential temperature and $\delta^{18}\text{O}$ from 15 m depth at the RaTS site during 2002 and 2003.

Figure 7. Locus of freshwater characteristics at the RaTS sampling site in salinity/ $\delta^{18}\text{O}$ space for 2002. Data points have been colour-coded according to time of year. Extrapolations between CDW and precipitation ($\delta^{18}\text{O} \approx -13\text{\textperthousand}$) and glacial meltwater ($\delta^{18}\text{O} \approx -20\text{\textperthousand}$) are marked, along with an approximate median line. Mixing of Marguerite Bay surface water with CDW would move the data points diagonally upward, along the line toward CDW. Mixing with meteoric water would move the points diagonally downward, along the line toward fresher, isotopically lighter waters. Sea ice processes (melting “M” and freezing “F”) would move the data points almost horizontally on this diagram.

Figure 8: As Figure 7, except for 2003.

Figure 9. Time series of percentages of meteoric water and sea ice melt for 15 m depth at the RaTS sampling site. Series were derived using $\delta^{18}\text{O}$ and salinity data processed according to equations 1-3. Note that the sea ice melt values are frequently negative; this indicates that a net sea ice formation had occurred from the waters sampled at these times.

Figure 10: Profiles of freshwater content (%) at the RaTS site derived from oxygen isotope and salinity data collected by *RRS James Clark Ross* during December 2001 (red), December 2002 (black) and December 2003 (blue). Dashed lines indicate meteoric water percentages, and solid lines indicate sea ice melt percentages. Note that negative sea ice melt percentages denote a net

sea ice formation had occurred from these waters. Total column inventories (H_{met} , H_{sim}) are shown for each year.

Figure 11: Seasonal progression of Precipitation (square), Evaporation (open circle) and Precipitation minus Evaporation (solid circle) averaged over Marguerite Bay (Van Lipzig *et al.*, 2004).

Figures

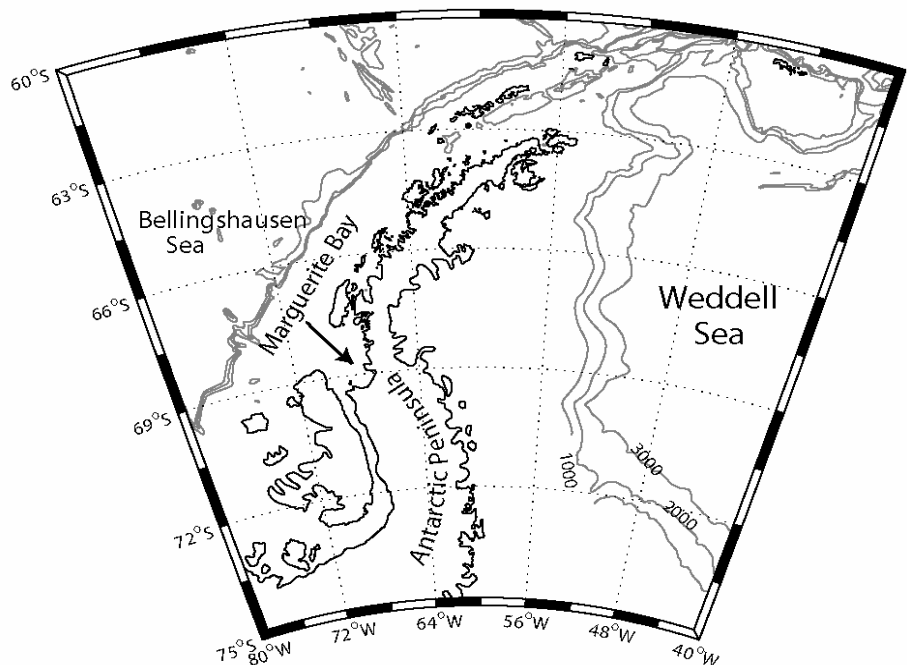


Figure 1. Location of Marguerite Bay on the Western Antarctic Peninsula. The 1000, 2000 and 3000 m isobaths are marked.

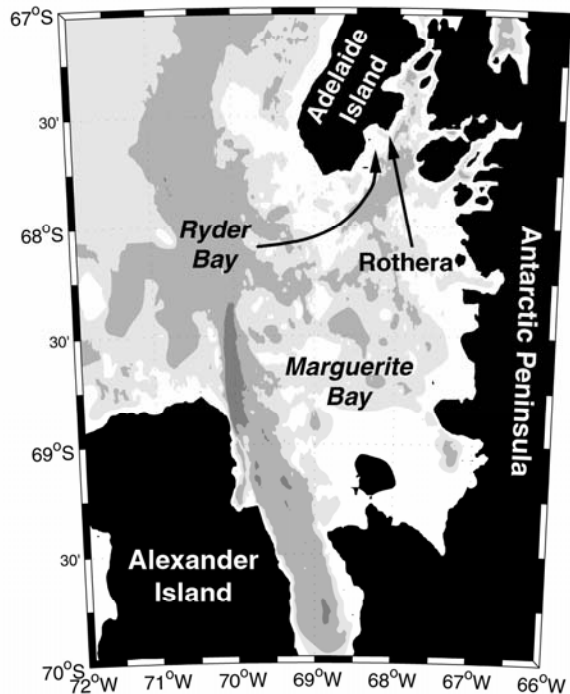


Figure 2. Bathymetry of Marguerite Bay, from the recently compiled SO GLOBEC bathymetric dataset. Shading denotes depths deeper than 1500 m (darkest), 1500-500 m, 500-250 m and shallower than 250 m (lightest). Marked are the British Antarctic Survey research station at Rothera on Adelaide Island, and the location of the Rothera Time Series (RaTS) sampling site in Ryder Bay.

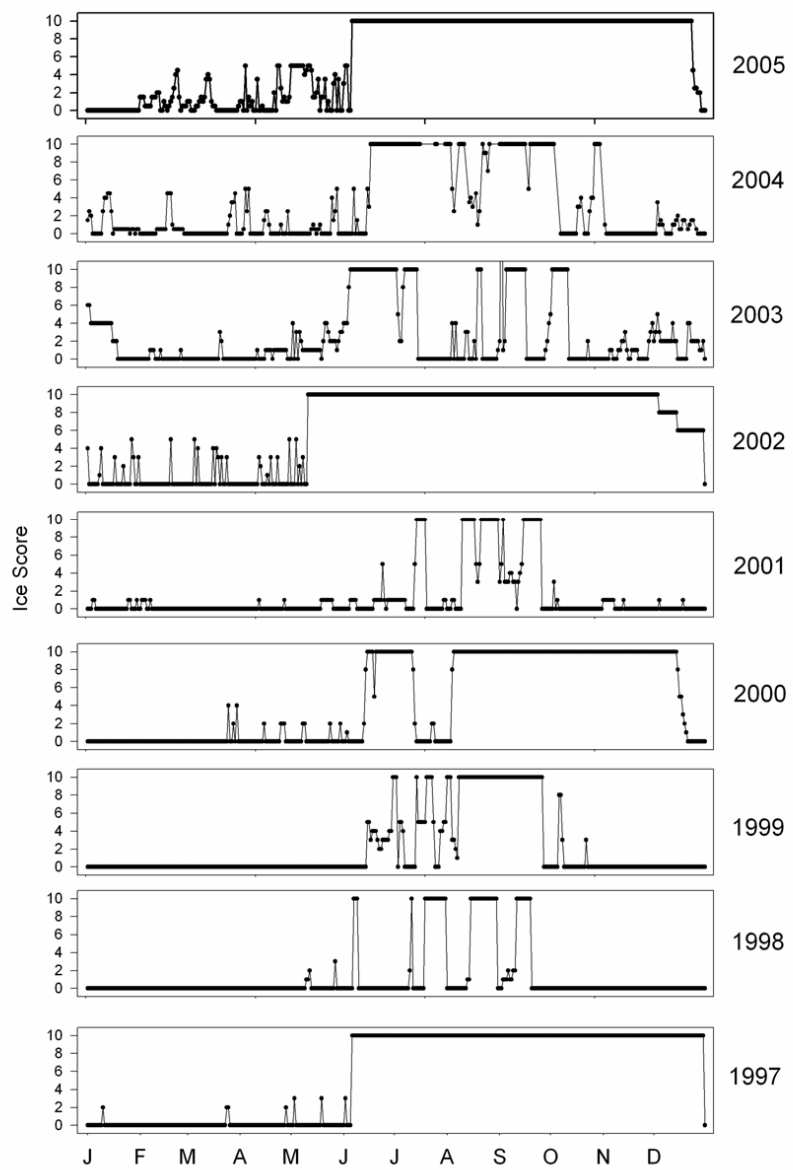


Figure 3. Winter fast-ice in Ryder Bay, northern Marguerite Bay, 1997-2006. Ice score ranges from 0 (open water) to 10 (complete fast ice cover). Data are plotted for the calendar year, so that winter lies in the centre of the plot. Figure reproduced from Clarke et al. (2007).

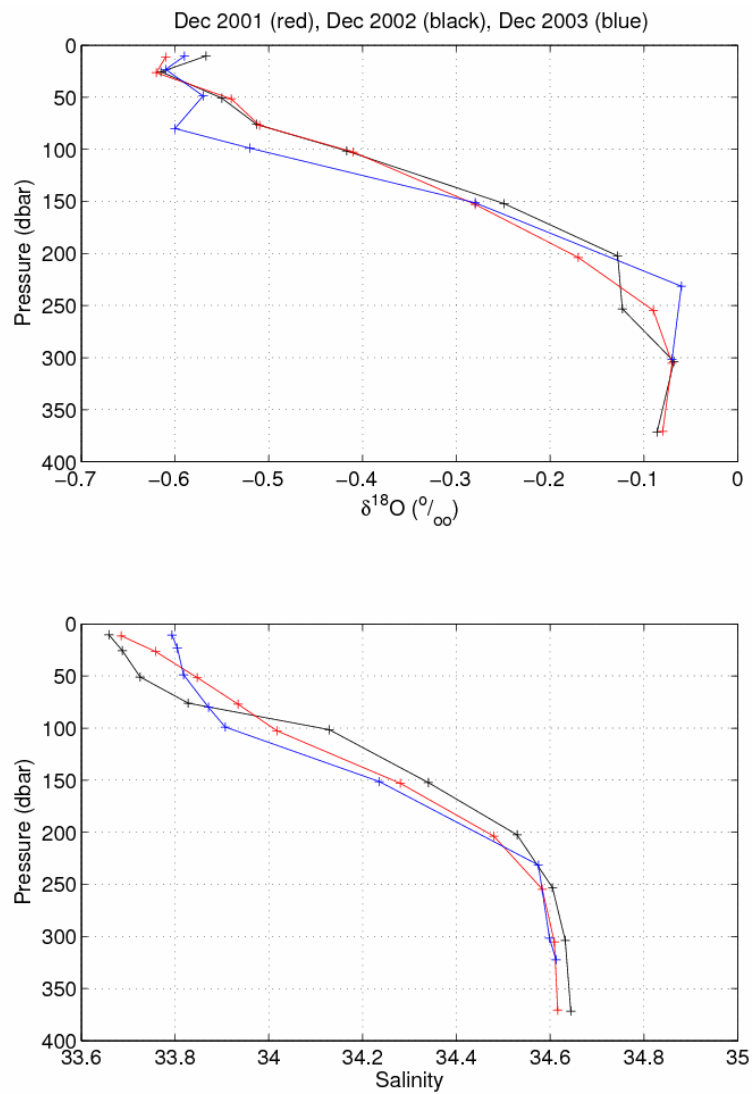


Figure 4: Vertical profiles of $\delta^{18}\text{O}$ and salinity obtained by CTD casts at the RaTS site conducted from *RRS James Clark Ross* during December 2001 (red), December 2002 (black) and December 2003 (blue).

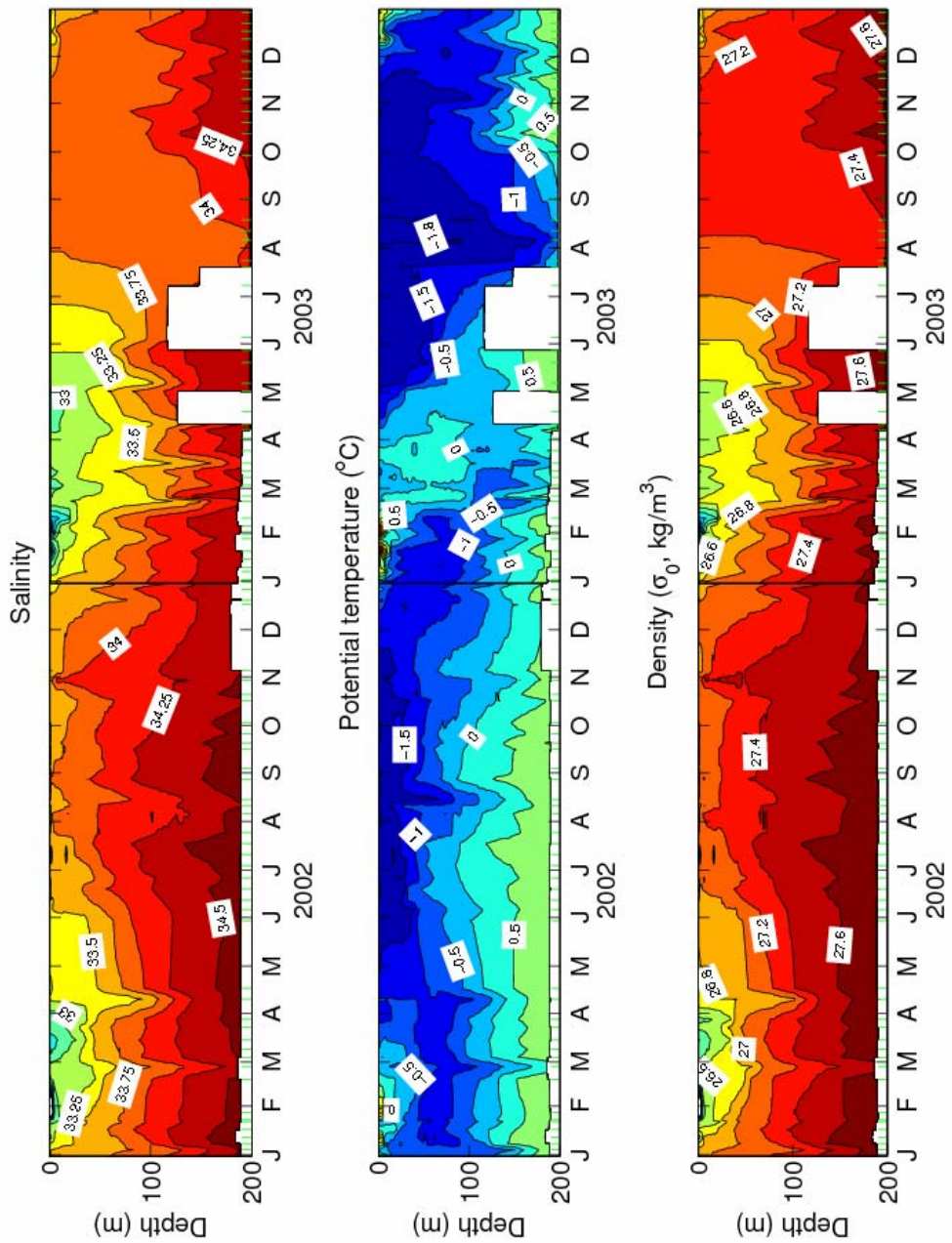


Figure 5: Time series of salinity, potential temperature ($^{\circ}\text{C}$) and density (σ_0 ; kg/m^3) for the upper 200 m of the water column during 2002 and 2003, from CTD casts conducted at the RaTS site.

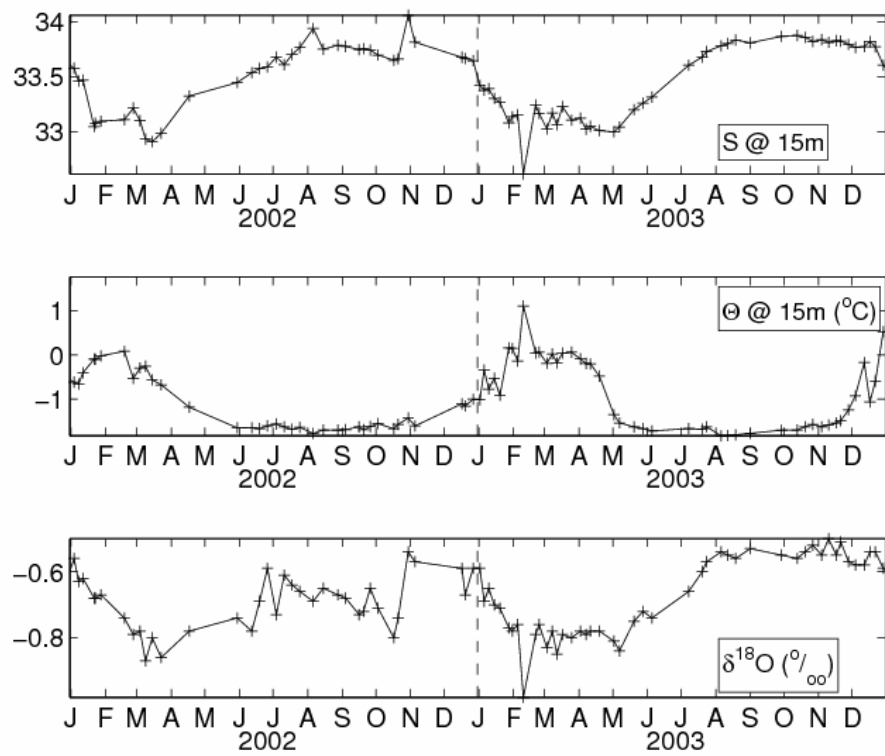


Figure 6: Time series of salinity, potential temperature and $\delta^{18}\text{O}$ from 15 m depth at the RaTS site during 2002 and 2003.

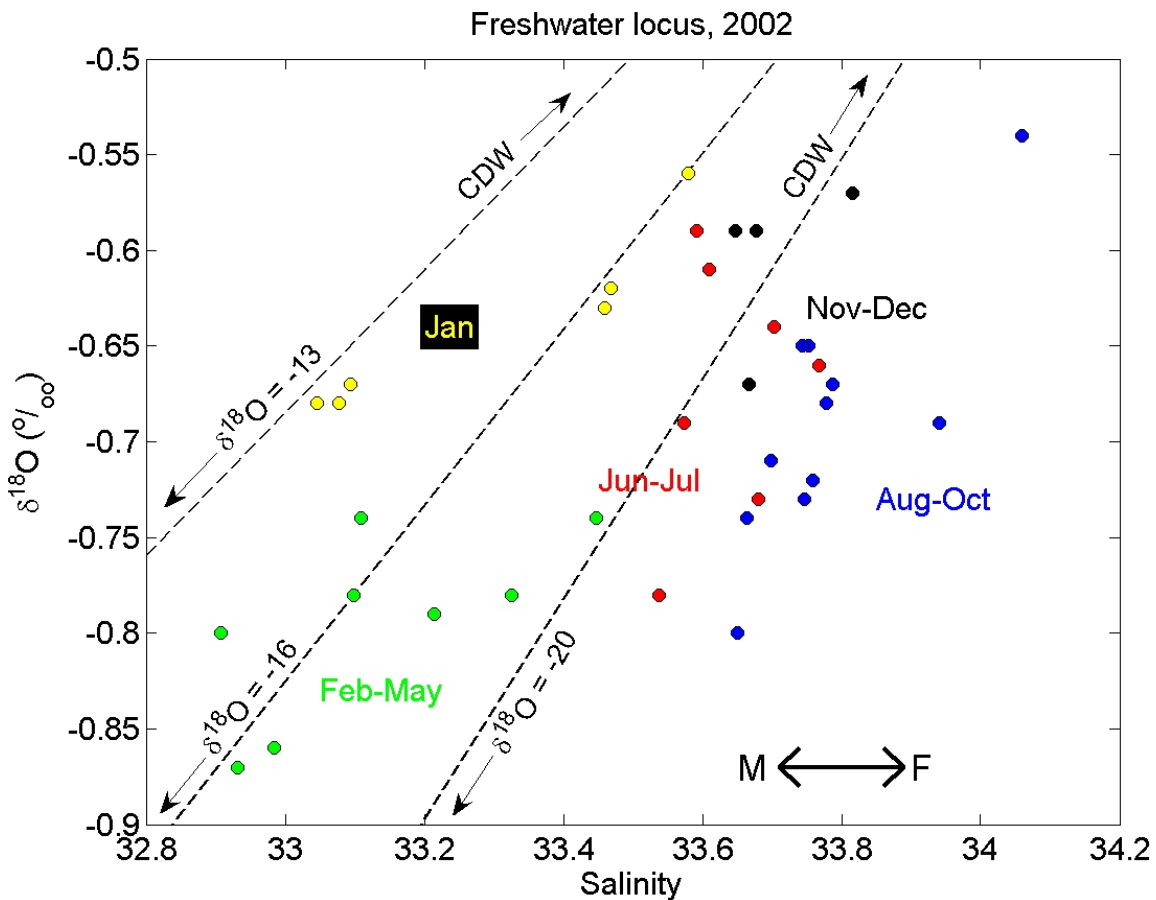


Figure 7. Locus of freshwater characteristics at the RaTS sampling site in salinity/ $\delta^{18}\text{O}$ space for 2002. Data points have been colour-coded according to time of year. Extrapolations between CDW and precipitation ($\delta^{18}\text{O} \approx -13\text{\textperthousand}$) and glacial meltwater ($\delta^{18}\text{O} \approx -20\text{\textperthousand}$) are marked, along with an approximate median line. Mixing of Marguerite Bay surface water with CDW would move the data points diagonally upward, along the line toward CDW. Mixing with meteoric water would move the points diagonally downward, along the line toward fresher, isotopically lighter waters. Sea ice processes (melting “M” and freezing “F”) would move the data points almost horizontally on this diagram.

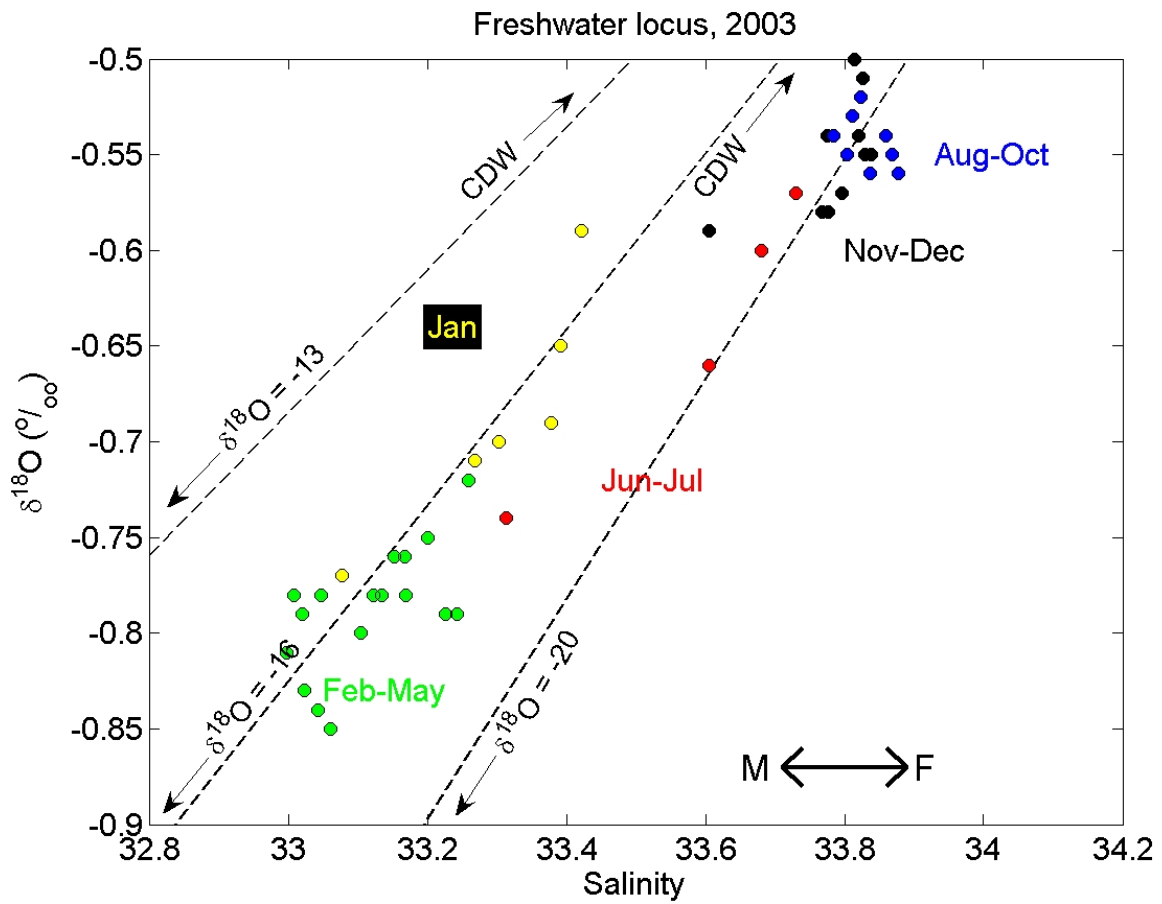


Figure 8: As Figure 7, except for 2003.

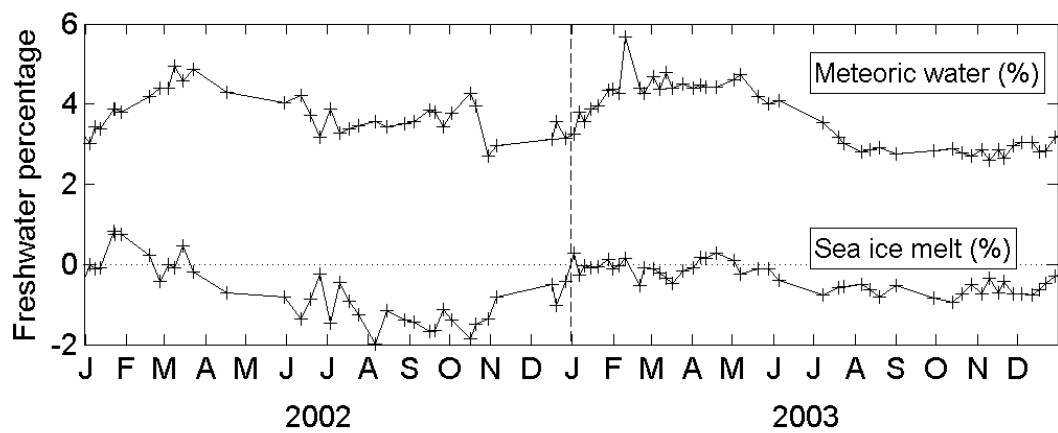


Figure 9. Time series of percentages of meteoric water and sea ice melt for 15 m depth at the RaTS sampling site. Series were derived using $\delta^{18}\text{O}$ and salinity data processed according to equations 1-3. Note that the sea ice melt values are frequently negative; this indicates that a net sea ice formation had occurred from the waters sampled at these times.

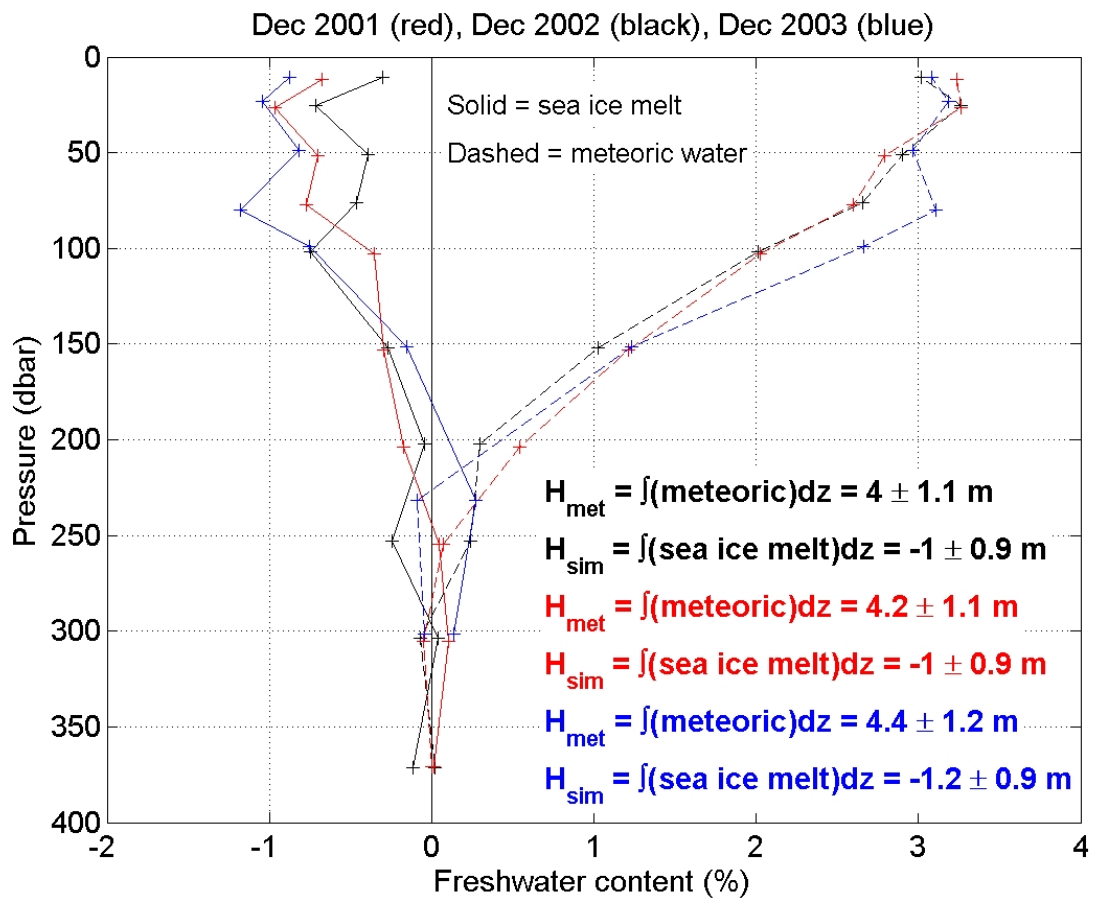


Figure 10: Profiles of freshwater content (%) at the RaTS site derived from oxygen isotope and salinity data collected by *RRS James Clark Ross* during December 2001 (red), December 2002 (black) and December 2003 (blue). Dashed lines indicate meteoric water percentages, and solid lines indicate sea ice melt percentages. Note that negative sea ice melt percentages denote a net sea ice formation had occurred from these waters. Total column inventories (H_{met} , H_{sim}) are shown for each year.

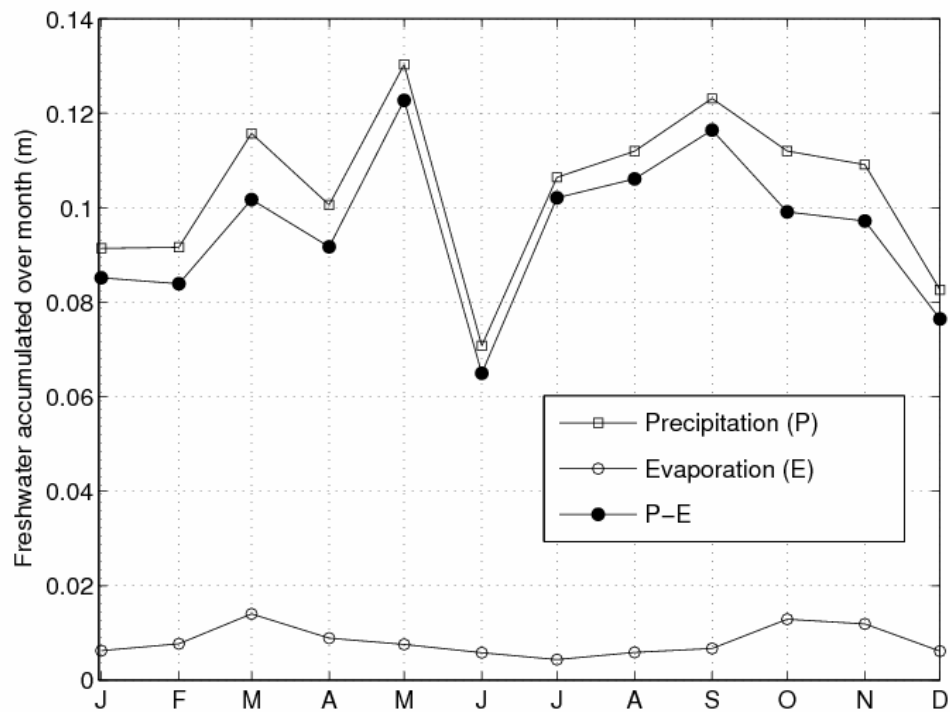


Figure 11: Seasonal progression of Precipitation (square), Evaporation (open circle) and Precipitation minus Evaporation (solid circle) averaged over Marguerite Bay (Van Lipzig et al., 2004).

Table 1. Values for endmembers used in mass balance calculations. Derivation of values is explained in the text.

	CDW	Sea ice melt	Meteoric Water
Salinity	34.62	7	0
$\delta^{18}\text{O}$ (‰)	-0.08	2.1	-17